the rotation potential is made steeper by ring clamping (compounds **1** and **2**) the agreement between calculated and experimental ring dihedral values improves significantly with respect to the unclamped situation. For all molecules the conformation around the central bond can always be described as approximately staggered. No geometrical parameters are reported in this paper for the phenyl rings. All the rings show slight distorsion with respect to hexagon symmetry. For unclamped rings the internal bond angle at the carbon connected to the ethane fragment is always calculated and found to be smaller than 120°, by a few degrees. The data are available from the authors, upon request. From the body of the results the general conclusion can be drawn that the EFF method is very reliable in the prediction of geometry for polyarylethylenes, giving support to the argument put forward by Mislow.[2] In fact, the average errors turned out to be 1.0% in bond lengths and 1.3% in bond angles.

The weakest points are the torsion around the central bond and the ring rotations. However, it must be remembered here that X-ray data describe the molecules packed in the crystal. Intermolecular forces come into play which may cause considerable change of these angles even when intermolecular atom-atom distances fall in the normal range. The suggestion can be made here that nonbonded intermolecular interactions should be included. Indeed preliminary calculations along these lines point in the right direction but for quantitative agreement an "ad hoc" parameterization of nonbonded intermolecular interactions, at variance with nonbonded intramolecular ones, should be performed. Work along these lines is actually in progress.

Acknowledgment. The authors are indebted to Drs. R. Bianchi, R. Destro, and A. Gavezzotti for helpful discussions.

Supplementary Material Available: Calculated and experimental geometrical parameters for the four molecules (Tables I, II, IV, and V) (4 pages). Ordering information is given on any current masthead page.

The Relationship between Nuclear Quadrupole Coupling Constants and the Asymmetry Parameter. The Interplay of Theory and Experiment

Jill E. Gready*

Contribution from the Physical Chemistry Laboratory, South Parks Road, Oxford, OX1 3QZ, United Kingdom. *Received September 23, 1980*

Abstract: A diagrammatic scheme is proposed for correlating assignments and orientations of the electric field gradient (EFG) components of nuclei in molecules. It is illustrated for oxygen in organic compounds and relies on an ordered, although not necessarily linear, relationship between ^{17}O nuclear quadrupole coupling constants and the asymmetry parameter recently noted for hydroxyl and carbonyl groups. All the available ^{17}O data from ab initio EFG calculations and NQR experiments on organic compounds are surveyed and integrated. The relative magnitudes of perturbations to the oxygen EFG components from differing substituents, intermolecular forces such as H bonding, and crystal lattice field effects are analyzed. Particular attention is given to correlating the EFG assignments and orientations of oxygen in the carboxyl and hydroxyl groups of carboxylic acids as, through increasing strength of H bonding, they become chemically equivalent in the limit of symmetrical H bonding as represented here by type A acid salts.

Introduction

The electric field gradients (EFG's) around nuclei in molecules have been shown by both theoretical[1-5] and experimental (chiefly NQR[6-8]) methods to be very sensitive to the chemical and physical environment of the nucleus, and hence their determination offers considerable potential to the chemist for studying bonding in compounds containing a given nucleus—for example, H, N, or O—in different functional groups or for varying substituents etc. This potential is hampered at present by problems in the extraction of complete EFG information from the available experimental data: specifically, it is difficult in many cases to establish the assignments and orientations of the EFG tensor with respect to molecular axes from NQR results. While quantum mechanical calculations can readily provide the assignments and orientations, the accuracy of the calculated coupling amplitudes is much less than can be obtained routinely by experiment. Few EFG results from gas phase (microwave spectroscopy) or liquid phase (NMR) are available, and hence separation of contributions to the measured solid-phase EFG's from intermolecular interactions such as H bonding and crystal-lattice perturbations is an additional problem.

Consequently the object of this paper is to propose a regime which utilizes the limited number of theoretical and gas-phase results in compiling graphs to correlate and analyze experimental data for the solid state: this procedure is illustrated for organic oxygen-containing compounds although it is expected to be applicable to other nuclei of major chemical interest such as nitrogen. The paper builds upon recent proposals of the existence of a

* Address correspondence to this author at the Department of Biochemistry, University of Sydney, N.S.W. 2006, Australia.

(1) Snyder, L. C.; Basch, H. "Molecular Wave Functions and Properties"; Wiley-Interscience: New York, 1972.
(2) Moccia, R.; Zandomeneghi, M. *Adv. Nucl. Quadrupole Reson.* **1975**, *2*, 135-178.
(3) (a) Olympia, P. L.; Fung, B. M. *J. Chem. Phys.* **1969**, *51*, 2976-2980. (b) Karlstrom, G.; Wennerstrom, H.; Jonssen, B.; Forsen, S.; Almlof, J.; Roos, B. *J. Am. Chem. Soc.* **1975**, *97*, 4188-4192.
(4) Gready, J. E. *Chem. Phys.* **1981**, *55*, 1-26.
(5) (a) Engstrom, S.; Wennerstrom, H.; Jonssen, B.; Karlstrom, G. *Mol. Phys.* **1977**, *34*, 813-821. (b) Engstrom, S.; Wennerstrom, H. *Ibid.* **1978**, *36*, 773-779.
(6) Redfield, A. G. *Phys. Rev.* **1963**, *130*, 589-595.
(7) (a) Slusher, R. E.; Hahn, E. L. *Phys. Rev. Lett.* **1964**, *12*, 246-248. (b) Slusher, R. E.; Hahn, E. L. *Phys. Rev.* **1968**, *166*, 332-347.
(8) (a) Edmonds, D. T. *Phys. Rep.* **1977**, *29*, 233-290. (b) *Bull. Magn. Reson.* **1981**, in press.
(9) Hsieh, Y.; Koo, J. C.; Hahn, E. L. *Chem. Phys. Lett.* **1972**, *13*, 563-566.
(10) (a) Kado, R.; Takarada, Y.; Halanaka, H. *Phys. Lett. A* **1974**, *47*, 49-50. (b) Kado, R.; Takarada, Y. *J. Magn. Reson.* **1978**, *32*, 89-91.
(11) Brown, T. L.; Cheng, C. P. *Symp. Faraday Soc.* **1978**, *13*, 75-82.

0002-7863/81/1503-3682$01.25/0

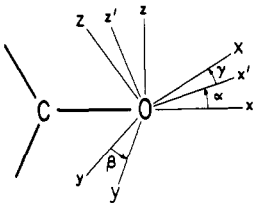

Figure 1. Schematic to show the relationship between molecular axes $\{x, y, z\}$ and principal axes $\{X, Y, Z\}$ via the Euler angles α, β, and γ. β represents the predominantly out-of-molecular plane rotation for A_aCOB_b systems in this work where "a" is usually 2 or 3 and "b" is usually 0 or 1.

relationship between e^2qQ/h and η values for ^{17}O nuclei in carbonyl-[12-14] and hydroxyl-containing compounds.[13,14] A refinement of the procedure is also applied to correlate the effects of H bonding on the EFG.

The recent advent of double[6-8] and triple[10] NQR techniques has allowed collection of data for the ^{17}O nucleus in natural abundance (0.037%). The organic O-containing compounds for which NQR data are available are listed in Table II:[9-16,21] a large number of carboxylic acids are represented.[11,13-16,21]

Introductory Theory and Definition of Problem

Computationally the electric field gradient (EFG) about a nucleus is characterized by six independent tensor components, eq_{xx}, eq_{yy}, eq_{zz}, eq_{xy}, eq_{xz}, and eq_{yz}, with respect to an arbitrary cartesian axis system $\{x, y, z\}$. Expectation values for these components are obtained by operating on the SCF wave function with an operator of the form, for example, for the eq_{zz} component about an oxygen nucleus, of

$$eq_{zz} = e\sum_N Z_N \frac{3z^2_{NO} - r^2_{NO}}{r^5_{NO}} - e\left\langle \psi \left| \sum_i \frac{3z^2_{iO} - r^2_{iO}}{r^5_{iO}} \right| \psi \right\rangle \quad (1)$$

where the index N is over all the other nuclei of charge Z_N, while "i" runs over all the electrons in the molecule. Diagonalization of the tensor produces traceless components eq_{ZZ}, eq_{YY}, and eq_{XX} as eigenvalues in the principal axis (PA) system $\{X, Y, Z\}$ while the eigenvector matrix specifies the rotation matrix between the $\{x, y, z\}$ and $\{X, Y, Z\}$ systems from which, by definition, the three Euler angles α, β, and γ can be derived.[17]

In nuclear quadrupole resonance the coupling between the nuclear quadrupole Q_O of the ^{17}O nucleus and the surrounding electric field gradient is measured by two quantities, the nuclear quadrupole coupling constant ν

$$\nu = (eq)(eQ/h) = e^2qQ/h \quad (2)$$

and the asymmetry parameter η

$$\eta = (eq_{XX} - eq_{YY})/eq_{ZZ} \quad (3)$$

Here eq corresponds to the largest component of the EFG tensor in the PA system which is labeled according to the convention $|eq_{ZZ}| > |eq_{YY}| > |eq_{XX}|$ (i.e., $eq = eq_{ZZ}$).

It is apparent from eq 1 that the EFG operator has a $1/r^3$ dependence. This is somewhat misleading because to first order[18] the inner regions of the electron distributions of most component atoms are essentially spherical, being little perturbed by the asymmetric bonding interactions, and their contribution to the total EFG averages to zero: in fact, the major contribution to the EFG around nuclei in molecules arises from the nuclear and electron distributions in the intermediate bonding regions—hence the sensitivity to chemical environment noted in the Introduction.

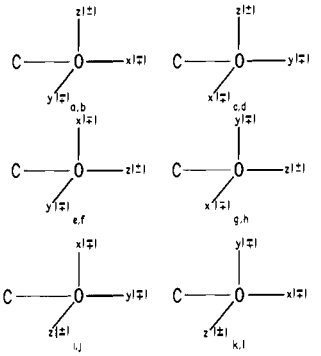

Figure 2. The twelve possible combinations of X, Y, and Z axes and signs for the EFG components of an oxygen nucleus for a *given* orientation of the PA system with reference to molecular axes—see Figure 4. For reference to coupling constant components in later figures all signs should be reversed (Q_O is negative).

It follows that in using EFG data to characterize and compare the electron/nuclear distributions about oxygen nuclei in a range of organic compounds it would be most desirable to know the values of eq_{ZZ}, eq_{YY}, and (by definition) eq_{XX} and the relationship of their principal axes to an arbitrary molecular axis system (Figure 1). However, the information available from most nuclear quadrupole double resonance experiments falls short of these criteria because (a) it is quite often not possible to determine the sign of e^2eQ/h and (b) the angular specification of the PA axes is usually imprecise, and assignment of the Z and, particularly, X and Y axes is not always unambiguous, and also (c) solid-phase EFG values include contributions from crystal lattice perturbations which may be interesting in themselves but which for purposes of comparing intramolecular bonding structure merely constitute physical noise.

In Figure 2 the twelve possible combinations of signs and assignments of X, Y, and Z axes are shown for *one* orientation of the $\{X, Y, Z\}$ axis system with respect to the "CO" bond in an organic molecule. There are indications from calculations[4] (see also Tables I and III) and experiment that for the two common functional groups C=O and C—OH, the orientations of the PA systems themselves with respect to the C—O bond direction are distinctly different. However, the orientations for a given functional group are relatively constant although the X, Y, and Z assignments vary.

Another current problem arises because computations of EFG's of moderate accuracy are restricted to small molecules, while most of the available experimental results on solids pertain to larger compounds: there is no example where computations, microwave and solid-phase data for the EFG's of an oxygen nucleus are all available. A recent computational paper[4] dealt at length with the ^2D and ^{17}O EFG's for H-bonded and non-H-bonded formic acid in gaseous and crystal phases, but unfortunately no gas-phase ^{17}O experimental results were available to critically assess the accuracy of the calculations and the specific contribution of solid-state effects. Use is made of the calculated and microwave ^{17}O EFG values for formaldehyde[22] in "standardizing" the computed values for a series of O-containing compounds (see Tables I and III) before use in the correlation graphs presented in later sections.

Theoretical Possibilities

In recent papers Cheng and Brown[12] and later Smith and Poplett[13,14,16] presented NQDR results supporting an almost linear relationship between e^2qQ/h and η for oxygen nuclei in both carbonyl and hydroxyl groups. As there is no purely *physical*

(12) Cheng, C. P.; Brown, T. L. *J. Am. Chem. Soc.* **1979**, *101*, 2327-2334.
(13) Poplett, I. J. F.; Smith, J. A. S. *J. Chem. Soc., Faraday Trans. 2* **1979**, *75*, 1703-1716.
(14) Smith, J. A. S. *J. Mol. Struct.* **1980**, *58*, 1-21.
(15) Brosnan, S. G. P.; Edmonds, D. T. *J. Magn. Reson.* **1980**, *38*, 47-63.
(16) Poplett, I. J. F. Ph.D. Thesis, University of London, 1979.
(17) A more detailed description of the computational procedure is given in ref 4.
(18) A second-order effect (Sternheimer shielding) arises from polarization of the electron distribution, particularly the inner shells, by the nuclear quadrupole itself: such contributions to the molecular e^2qQ/h values are usually small.
(19) Berglund, B.; Lindgren, J.; Tegenfeldt, J. *J. Mol. Struct.* **1978**, *43*, 179-191.
(20) Poplett, I. J. F.; Smith, J. A. S. *J. Chem. Soc., Faraday Trans. 2* **1981**, in press.
(21) Brosnan, S. G. P. D.Phil. Thesis, University of Oxford, 1980.
(22) Flygare, W. H.; Lowe, J. T. *J. Chem. Phys.* **1965**, *43*, 3645-3653.

Table I. Comparison of EFG Components for Some Carbonyl Compounds

molecule[a]	q_{ZZ}, au	q_{YY}, au	q_{XX}, au	$e2qQ/h$,[e] MHz	η[d]	θ,[c] deg	p_π
H_2CO (VII)	−2.612	1.916	0.697	16.27	0.467	90.0	1.293
$H_2C(CH)_2O$ (XIII)	−2.502	1.663	0.839	15.58	0.330	90.7	1.338
HFCO (VIII)	−2.213	1,425	0.788	13.78	0.288	88.2	1.352
F_2CO (IX)	−2.179	1.154	1.025	13.57	0.059	90.0	1.378
HCOOH (III)[b]	−2.169	1.132	1.037	13.51	0.044	87.8	1.434
HCOOH (III)	−2.087	1.093	0.994	13.00	0.047	89.1	1.434
	q_{ZZ}	q_{XX}	q_{YY}				
HNH_2CO	−2.081	0.996	1.085	12.96	−0.043	(89.4)	1.451
$(HCOOH)_2$ (VI)[b]	−1.829	0.709	1.120	11.39	−0.224	90.7	1.536
$HCOO^-$ (V)	−1.742	0.420	1.322	10.85	−0.518	90.5	1.622
	q_{XX}	q_{ZZ}	q_{YY}				
H_2CCO (XI)	0.763	−1.550	0.787	−9.65	0.016		1.425

[a] Values from ref 1 except *b*. [b] Values from ref 4. [c] Anticlockwise angle of rotation of in-plane PA's with respect to C→O bond for configurations shown in Figure 4 required to specify orientation of the *Z* axis. Approximate value for nonplanar system X – ref 4. [d] Definition of sign as for Figure 3. [e] Calculated by using the conversion factor 1 au = −6.227 MHz obtained by assuming $Q_O = -0.0265$ barn.[44]

reason why changes in e^2qQ/h amplitude should be accompanied by any particular pattern of variation in the other two components, it must be assumed that the regularity is due to an as-yet-poorly-characterized conservation property of the chemical bond. The aim here is to explore the relationship further for carbonyl and hydroxyl groups by considering additional experimental data and to test its generality by extension to other oxygen-containing groups and H-bonding environments.

The major features of the type of extended correlation diagram proposed in this work are illustrated in Figure 3. Figure 3 represents the possible relationships between all the hypothetical assignments of tensor components shown in Figure 2 for the carbonyl group, although it is not necessarily suggested that examples of carbonyl-containing compounds do or should exist for all branches of this diagram. Several general aspects of the diagram require explanation. First, it differs from those previously published[12-14] in having both positive and negative axes for e^2qQ/h and η; i.e., it has four quadrants instead of one. The major advantage of the expanded representation is that it allows "pathways" whereby one assignment changes into another to be determined by inspection: $X \leftrightarrow Y$ interchanges occur at $\eta = 0$ and involve no sign change for e^2qQ/h, while $Z \leftrightarrow Y$ interchanges occur at $\eta = \pm 1$ and *necessarily* involve a sign change for e^2qQ/h. The "sign" of η is established arbitrarily for one assignment—for example, in Figure 3 η is chosen to be positive for assignment b (Figure 2)—thereby fixing the signs of all other possible assignments.

In Figure 3 the positions (and slope) of lines b and d represent the best fit to the experimental data found previously[16] while the EFG assignments (i.e., b and d from Figure 2) have been made on the basis of theoretical results presented in the following sections. At present there are no experimental or theoretical data to justify the magnitude or sign of the slopes of the other lines: establishing the positions of these other branches of the diagram awaits the availability of data for a wider range of carbonyl compounds. For emphasis on the tentativeness of these details, some dashed lines of negative slope have been drawn in addition to the solid lines which depict slope behavior extrapolated from that found for *some* carbonyl compounds (i.e., lines **b** and **d**).

A final point: using trial values it is easy to show that a decrease in e^2qQ/h *may* be accompanied by either an increase or a decrease in $|\eta|$ depending on the relative change in the quantity $eQ/h(eq_{XX} - eq_{YY})$. Consequently a plot of e^2qQ/h vs. $eQ/h(eq_{XX} - eq_{YY})$ may prove to be a more direct means of representing the changes in the EFG components and crossover points which accompany variation in the chemical environment of the nucleus.

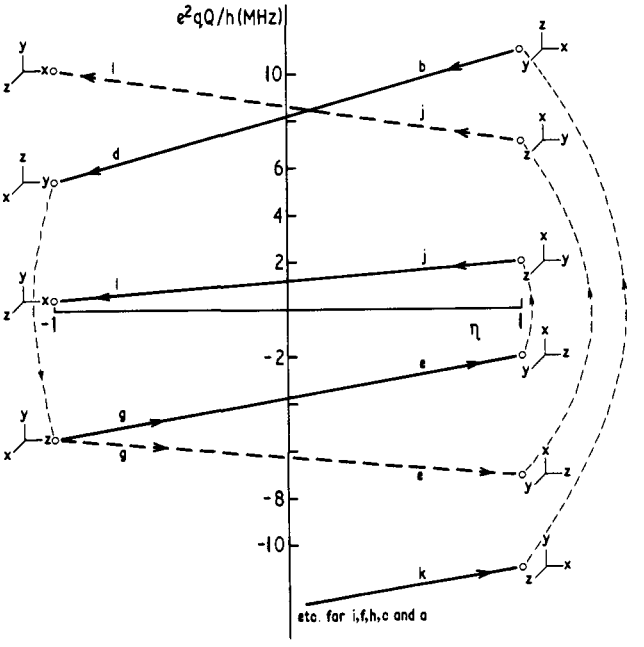

Figure 3. General e^2qQ/h vs. η diagram showing "pathways" for all possible interconversions between EFG assignments for the carbonyl group. Solid lines represent behavior demonstrated for a restricted class of compounds as shown in lines b, d, and possibly g. Dashed lines represent examples of behavior of opposite slope. Letters refer to assignments shown in Figure 2.

Theoretical Results for O-Containing Compounds

The computational literature on oxygen EFG's in molecules is limited.[1,2,4] A number of results for carbonyl-containing compounds are plotted in Figure 5 together with those of some other compounds including two with hydroxyl groups (CH_3OH and HCOOH). For a comparison to be facilitated with the experimental e^2qQ/h vs. η graphs, Figure 5 has been drawn with the EFG axis inverted (note that Q_O is negative; see Table I, footnote *e*), The calculated EFG values for the carbonyl compounds together with the orientation (θ) of the principal component with respect to the C=O bond (i.e., all approximately 90°) are listed in Table I while the corresponding assignments are indicated in Figure 4, The corresponding values for the hydroxyl compounds are given in Table III. Where necessary the quoted values have been obtained after the complete EFG tensors given in ref 1 are diagonalized.

For the carbonyl data reference to Figure 5 shows an orderly decrease of e^2qQ/h with decreasing η, although the relationship is not unambiguously linear. However, the approximate fit is more striking if the positions of the noncarbonyl points are considered. The dashed lines drawn through the two hydroxyl compounds (I and II) represent a preliminary correlation between the two assignments which is supported by the experimental data given in Figure 6.

Correlation of Carbonyl and Hydroxyl Data

In Figure 6 all the available theoretical and experimental ^{17}O data for carbonyl and hydroxyl groups in organic compounds are

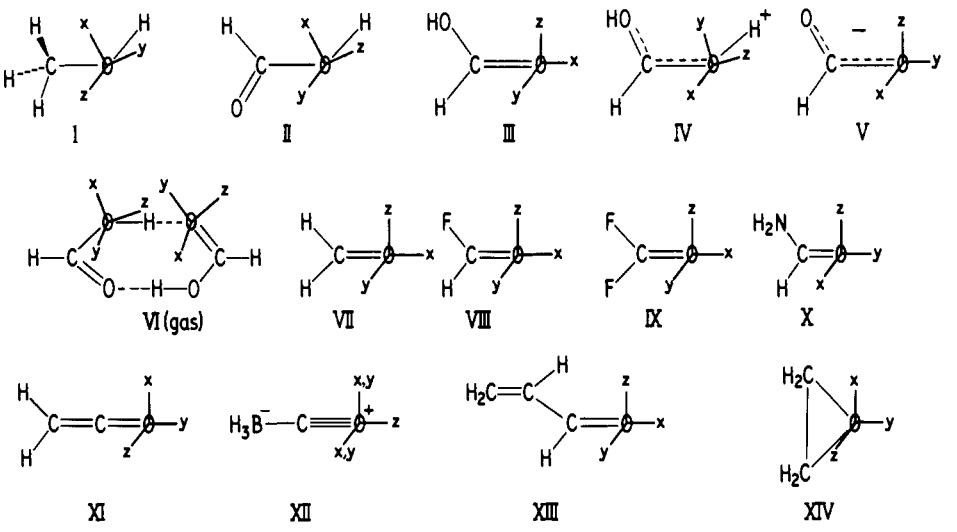

Figure 4. Orientations of the principal axes with respect to molecular axes corresponding to the computed oxygen EFG values of a number of organic molecules given in Tables I and III.

Table II. ^{17}O Experimental References

compd	ref	compd	ref	compd	ref
benzoic acid (1)	16	potassium hydrogen diformate (23)	16	benzyl chloroformate (45)	12
p-chlorobenzoic acid (2)	16	potassium hydrogen oxalate (24)	16	acetic acid (46)	52
m-chlorobenzoic acid (3)	16	potassium hydrogen phthalate (25)	16, 12	phenyl benzoate (47)	12
p-nitrobenzoic acid (4)	16	sodium formate (26)	12	benzoic anhydride (48)	12
m-nitrobenzoic acid (5)	16	potassium hydrogen maleate (27)	13	phthalic anhydride (49)	12
o-nitrobenzoic acid (6)	16	rubidium hydrogen maleate (28)	13	maleic anhydride (50)	12
aspirin (7)	16	potassium hydrogen chloromaleate (29)	13	chloroacetic anhydride (51)	12
p-hydroxybenzoic acid (8)	16	potassium hydrogen dibenzoate (30)	16	phthalimide (52)	12
m-hydroxybenzoic acid (9)	16	potassium hydrogen bis(*p*-chlorobenzoate) (31)	16	phthalide (53)	12
salicylic acid (10)	16	potassium hydrogen bis(*m*-chlorobenzoate) (32)	16	*p*-benzoquinone (54)	9
phthalic acid (11)	16	potassium hydrogen diaspirinate (33)	16	2,5-dichloro-*p*-benzoquinone (55)	9
isophthalic acid (12)	16	benzoyl fluoride (34)	12	2,6-dichloro-*p*-benzoquinone (56)	9
β-oxalic acid (13)	16	benzoyl chloride (35)	12	2,3-dichloro-1,4-napthoquinone (57)	9
maleic acid[a] (14)	21	4-chlorobenzoyl chloride (36)	12	1,5-dichloroanthraquinone (58)	9
maleic acid[a] (15)	21	4-chlorobenzaldehyde (37)	12, 10a	tetrachlorohydroquinone (59)	9
α-oxalic acid (16)	21	4-nitrobenzaldehyde (38)	12	2,5-dichlorohydroquinone (60)	9
acrylic acid (17)	21	3-nitrobenzaldehyde (39)	12	*p*-chlorophenol (61)	10a
fumaric acid (18)	21	benzoyl cyanide (40)	12	*m*-chlorophenol (62)	10b
formic acid (19)	15, 11	4,4'-dichlorobenzophenone (41)	12	*m*-chlorobenzaldehyde (63)	10b
ethanediol (20)	15	benzophenone (42)	12	dichloroacetone (64)	10b
phenol (21)	11	4-chlorobenzophenone (43)	12	xanthene (65)	9
2,6-dichlorophenol (22)	16	benzoyl peroxide (44)	12		

[a] Inequivalent carboxylate groups; see text.

plotted. The numbering for the experimental points corresponds to the compound list in Table II. The theoretical points refer to the molecules previously plotted in Figure 5, but the e^2qQ/h values (in MHz)—but not the η values—have been scaled before being replotted because the computed e^2qQ/h values are uniformly too high compared with experiment.[2,4] As ^{17}O gas-phase experimental data are available for only one organic molecule—formaldehyde ($e^2qQ/h = +12.37 \pm 0.01$ MHz, $\eta = 0.69$[22])—all the carbonyl and hydroxyl theoretical e^2qQ/h values were scaled against the formaldehyde theoretical/experimental values. However, the quantitative validity of the scaling over the complete range of molecules is clearly questionable. As defined in the figure caption, the plotted points correspond to oxygen nuclei involved in asymmetric or symmetric H bonding or no H bonding. For clarity and easy reference in the following discussion additional qualitative features of Figure 6 are depicted in a condensed form in Figure 7. In this discussion the general features for each group will be noted first followed by analysis of the specific effects of H bonding and examination of example compounds.

As noted in Theoretical Possibilities construction of the e^2qQ/h vs. η graph required a preliminary arbitrary choice of positive η axis for a given EFG assignment. However, for the present case of data for two groups being plotted on the same graph choice of the positive η axis for the second group may be guided by

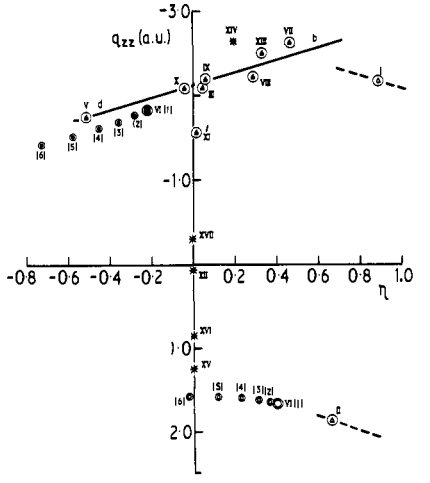

Figure 5. Plot of q_{zz} vs. η for computed oxygen values given in Tables I and III. Circled ▲ and ● refer to non-H-bonded and H-bonded carbonyl groups, respectively. Circled △ and ○ refer to non-H-bonded and H-bonded hydroxyl groups, respectively. The asterisk refers to miscellaneous O-containing compounds. Points **1–6** refer to the model calculations for the formic acid dimer; see Effects of H Bonding and Table IV.

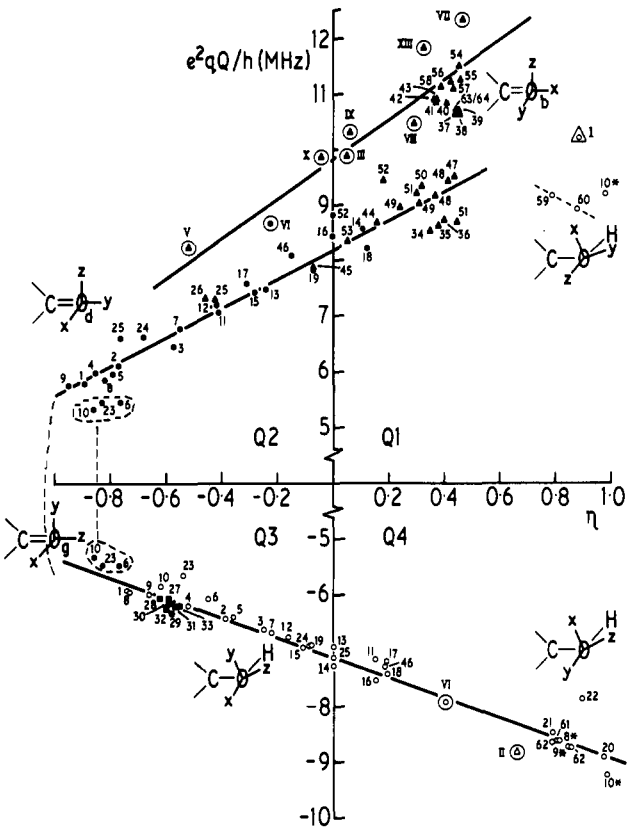

Figure 6. e^2qQ/h vs. η graph representing available ^{17}O theoretical and experimental data for carbonyl- and hydroxyl-containing compounds as referenced in Tables I–III. ●, ▲, ○, and △ represent experimental points for asymmetric H-bonded and non-H-bonded carboxyl groups and asymmetric H-bonded and non-H-bonded hydroxyl groups, respectively, while circled ●, ▲, ○, and △ represent the corresponding theoretical results. ■ represents the experimental values for symmetrically H-bonded oxygen. For experimental temperatures see references in Table II.

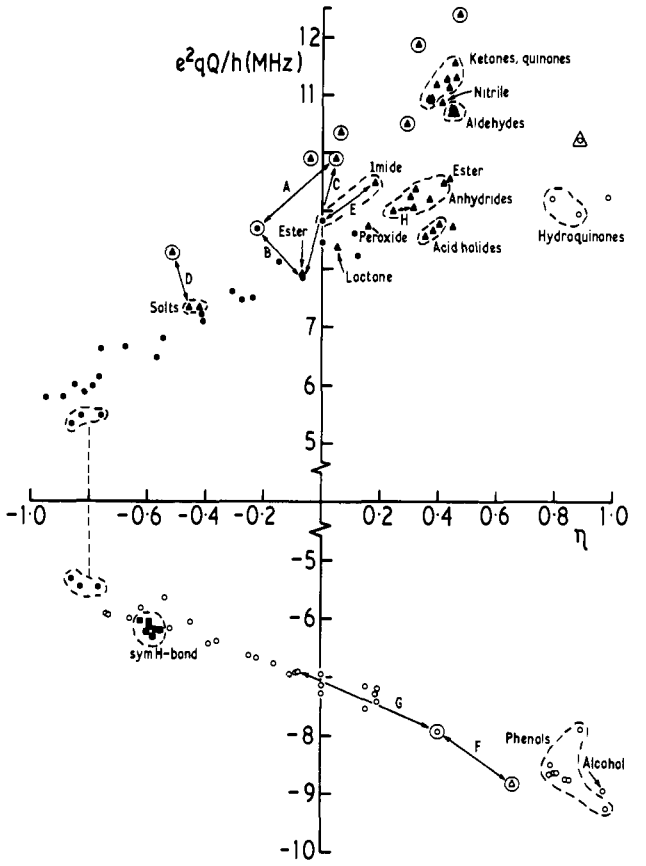

Figure 7. Condensed version of Figure 6 illustrating a number of qualitative features described in the text.

subsequent ease in illustrating interrelationships between the assignments for the two groups. In Figure 6 the motive was to demonstrate a correlation in the assignments and orientations of the EFG's of the oxygen nucleus in symmetrically H-bonded acids with those for the asymmetrically H-bonded carboxyl and hydroxyl groups to which they are related by necessary local symmetry constraints (see Effects of H Bonding).

Carbonyl Group. Considering first the carbonyl group and ignoring for the present the effects of H bonding, it may be seen that the experimental points in quadrants 1 and 2 conform well to a linear relationship. Of the types of carbonyl compounds represented in Figure 7, it is seen that the carboxylic acids, anhydrides, esters, salts, and peroxide deviate least from the line as drawn, while the acid halides lie slightly below it, the imide slightly above it, and the ketones, aldehydes, and nitriles yet higher. Comparison with the scaled (Figure 6) and unscaled (Figure 5) theoretical lines indicates similar qualitative deviations for the aldehyde (HCHO; VII) and acyl fluoride (HCOF; VIII). Obviously placement of the experimental line has been biased by the comparatively large number and spread of points representing the CO– group in the carboxylic acids and hence the implication of "deviation" is relative only. Nevertheless it is apparent that, at least for a range of coupling constant values between ~5.75 and 9.5 MHz, compounds of the form R—C(=O)—(O) conform well to the linear relationship.

The evident grouping of values for the aldehydes, and ketones and quinones, in particular, in Figure 7 requires some comment as it appears to conflict with the present thesis that sensitivity to chemical environment will lead to a spread of e^2qQ/h and η values for any particular class of compounds. Indeed, the initial conclusion of Hsieh et al.[9] based on the earliest ^{17}O results for the quinones (**54–58**) and hydroquinones (**59** and **60**) was that the e^2qQ/h and η values were characteristic for a given intramolecular bond structure, with solid-state and nearest-neighbor effects being of secondary importance. This contention has not been supported by the subsequent results for the carboxylic acids, esters, or anhydrides (Figure 7). It is probable that the clustering of values merely reflects the close chemical similarity of most of the (aromatic) ketone and aldehyde examples plotted in Figures 6 and 7. Inspection of the values for meta and para isomers among the acids supports this contention. The presence or absence of H bonding per se does not appear to affect this conclusion, although there are suggestions (see Effects of H Bonding) that differing strengths of H bonds may tend to spread the values for otherwise very similar compounds.

The assignments (**b** and **d**) for quadrants 1 and 2 were obtained from calculations (Figure 4). The validity of these assignments for the experimental points depends on the close analogy between the experimental and theoretical lines. The difference between the positions and slopes of the (scaled) theoretical and experimental lines is attributed mostly to crystal field effects: the magnitude of this effect is illustrated for formate (V) and formic acid (VI) by lines D and B in Figure 7. Another general point concerns carbonyl points 10, 23, and 6 which are plotted twice in Figure 6: as plotted in the 2nd quadrant they are seen to deviate significantly from the line, while as plotted in the 3rd quadrant a change in the EFG assignments is indicated (from d to g).

Finally on general points it is appropriate to comment on any variations in the orientation of the PA system itself for the carbonyl group represented in such a wide range of chemical environments. The orientation drawn in Figure 2 shows one axis coincident with the bond and one perpendicular to it in the same plane as the two carbon substituents (i.e., sp^2 bonding), while the third is necessarily perpendicular to the molecular plane. Reference to Tables I and III indicates that this orientation is approximately constant for the isolated molecules (see footnote *c*), but, more significantly, it has also been found for both the in-plane and out-of-plane H-bonded carboxyl groups in gaseous and crystalline formic acid.[4] This constancy contrasts with that found for the hydroxyl group as discussed below. The above discussion ignores any as-yet-

Table III. Comparison of EFG Components for H-Bonded and Non-H-Bonded Formic Acid and Also Methanol

molecule[a]	oxygen	q_{ZZ}, au	q_{YY}, au	q_{XX}, au	e^2qQ/h,[g] MHz	η[c]	θ,[d] deg
HCOOH (III)	C=O	−2.169	1.132	1.037	13.5	0.044	87.8
$(HCOOH)_2$ (VI)	C=O	−1.829	0.709[e]	1.120[e]	11.4	−0.224	90.7
HCOOH (II)	C–O	1.864	−1.548	−0.316	−11.6	0.661	−35.1
$(HCOOH)_2$ (VI)	C–O	1.662	−1.163	−0.499	−10.4	0.399	−22.7
H_3COH (I)[b]	C–O	2.031[f]	−2.155[f]	0.124	13.4	0.885	(−32.7)
$HCOOH_2^+$ (IV)[h]	C–O	1.878	−1.456	−0.422	−11.7	0.550	−30.3
$HCOOH_2^+$ (IV)[h]	C=O	1.506	−0.613[i]	−0.894[i]	−9.4	−0.186	−28.9

[a] Values from ref 4 except *b*. [b] Values from ref 1. [c] Definition of sign as for Figure 6. [d] See Table I, footnote *c*. Approximate value for CH_3OH–see ref 4. [e] Note the $q_{YY} \leftrightarrow q_{XX}$ interchange compared with III. [f] Note the $q_{ZZ} \leftrightarrow q_{YY}$ interchange compared with II. [g] See Table I, footnote *e*. [h] Model calculation for protonated species (see ref 4): carboxyl oxygen now resembles hydroxyl oxygen. [i] Note the $q_{YY} \leftrightarrow q_{XX}$ interchange compared with II.

uncharacterized perturbations to the orientation by specific crystal field environments.

Hydroxyl Group. In comparison with the variety of both experimental and theoretical ^{17}O data for the carbonyl group, that presently available for the hydroxyl group is more limited: computed ^{17}O hydroxyl values for methanol (I) and formic acid (II and VI) are plotted in Figure 6 while the experimental points refer mostly to the H-bonded group in carboxylic acids together with a few values for H-bonded phenols and hydroquinones, while there is only one example of an alcohol (ethanediol; **20**). When the presence or absence of H bonding is disregarded, the experimental OH points in Figure 6 are seen to obey an approximately linear relationship. The values for the phenolic group of salicylic acid (no. 10*) have been plotted twice to point out two possible assignments (1st and 4th quadrants) both of which are in harmony with the general OH line: it should be noted that this group is involved in a very unusual tightly bound intramolecular H bond bent with an angle of ~145° at the hydrogen.[23] The $|e^2qQ/h|$ values for the hydroquinones (**59** and **60**) are below the line projected from the 4th to the 1st quadrants. In the absence of a crystal structure for ethanediol it is assumed that the hydroxyl group is H bonded. As for the computed carbonyl values, those for the hydroxyl group were scaled against those for formaldehyde: the unscaled values are quoted in Table III.

The assignments of the PA's shown for the OH group in quadrants 1, 3, and 4 are derived by analogy with the assignments computed for formic acid (II and VI) and methanol (I). The angle between the Z axis and the C–O bond in formic acid was calculated[4] as ~35° in the direction indicated in Figure 4, while a similar orientation, but with a changed assignment, is calculated for methanol. Also, the results of the recent study[4] show that H bonding of the OH group in formic acid lowers this angle to ~23° in contrast to the negligible H-bond shift for the carbonyl group PA orientation previously noted. These results are summarized in Table III. It should be noted that the assignment and orientation indicated for the phenols (4th quadrant) are distinctly different from those previously proposed.[13]

Effects of H Bonding

In this section the general conclusions presented in Correlation of Carbonyl and Hydroxyl Data are refined to include the specific perturbations of the oxygen EFG's by H bonding. Some pertinent results of the recent study of the effect of H bonding on the carboxyl and hydroxyl oxygen EFG's of formic acid are summarized in Table III. Here it is seen that H bonding lowers both the carboxyl and hydroxyl $|e^2qQ/h|$ and η values: for the carboxyl group the shift involves an interchange of the X and Y axes. These shifts are represented by lines A and F in Figure 7. The present scarcity of other experimental or theoretical data for both H-bonded and non-H-bonded forms of the same (or very similar) compounds hampers the assessment of the generality of these trends, but it is encouraging that the same trend for the carbonyl group is shown by the one available experimental example—phthalimide (**52**; line E on Figure 7). In phthalimide one of the two chemically equivalent carbonyl groups is H bonded while the other is not.[11,24] The possibility that part of this shift may be due to differing crystal site effects must also be considered: however, if the magnitude of these effects is of the same order as that observed for the two non-H-bonded carbonyl groups in phthalic anhydride (**49**; line H in Figure 7), then the likelihood of the phthalimide shift being mostly due to specific H bonding is increased.

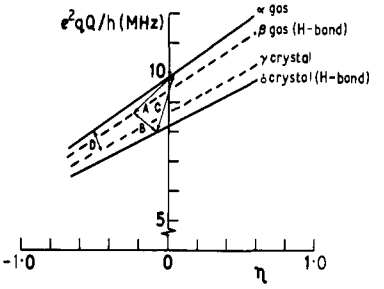

Figure 8. Schematic representation of the relationship between e^2qQ/h vs. η graphs for the carboxyl group in differing intermolecular environments.

Figure 8 is a nonquantitative representation of the expected directions of the H-bonding and/or crystal field shifts for the carbonyl group in a given class of compounds, e.g., carboxylic acids. An additional point not shown is that while for a given oxygen nucleus in any particular compound it is expected that either H-bonding or crystal effects will lead to a lowering of $|e^2qQ/h|$, the direction of the accompanying shift in η is less easy to predict.

Symmetric H Bonding in Carboxylic Acids. The ^{17}O coupling constant values[13,16] for those oxygen nuclei in type A salts thought to be involved in symmetric H bonding[25] are seen in Figure 6 to be strongly grouped: this clustering together with similarly apparently characteristic ^2H values for the H-bonded proton has been discussed previously.[13] While the sign of e^2qQ/h or the assignment and orientation of the PA system for these ^{17}O values have not yet been established experimentally, the assumption and use of a correspondence-type principle proposed below allow these to be deduced. The experimental and theoretical basis for this scheme is discussed first.

Although asymmetric H bonding of a carboxylic acid involves both electronic and structural (i.e., bond length and angle) changes in the vicinity of the carboxylic acid oxygen nuclei, the molecule still contains carboxyl and hydroxyl groups which are identifiable by spectroscopic and other methods. Thus, in comparison with the absolute differences between the EFG values and orientations for the non-H-bonded carboxyl and hydroxyl oxygen nuclei in formic acid, the perturbations introduced by H bonding are relatively small (Table III and Figure 6). Ionization of the isolated acid produces chemical equivalence of the two oxygens although asymmetry in the crystal geometry may introduce a degree of inequivalence in the C–O bond lengths and angles. The computed EFG results for the formic acid/formate pair indicate that the oxygen nuclei in the anion resemble those of the acid carboxyl group rather than the hydroxyl oxygen (Figure 4 and Tables I

(23) Bacon, G. E.; Jude, R. J. *Z. Kristallogr.* **1973**, *138*, 19–40.

(24) Matzat, E. *Acta Crystallogr., Sect. B* **1972**, *B28*, 415–418.

(25) (a) Speakman, J. C. *Struct. Bonding (Berlin)* **1972**, *12*, 141–199. (b) *MTP Int. Rev. Sci.: Inorg. Chem., Ser. Two* **1975**, *11*, 1–20.

Table IV. Trends in ^{17}O e^2qQ/h and η Values for Gradual Formation of a Symmetric H Bond in Model Calculations of the Formic Acid Dimer

calcn	group	r_{O-H},[a] Å	q_{ZZ}, au	q_{YY}, au	q_{XX}, au	e^2qQ/h, MHz	η[b]	θ,[c] deg
1	C=O	1.664	−1.829	1.119	0.710	11.39	−0.224	90.7
	C−O	1.058	1.663	−1.164	−0.499	−10.35	0.400	−22.7
2	C=O	1.611	−1.764	1.132	0.632	10.98	−0.283	91.7
	C−O	1.111	1.637	−1.117	−0.520	−10.20	0.365	−21.5
3	C=O	1.558	−1.690	1.148	0.543	10.52	−0.358	92.8
	C−O	1.164	1.613	−1.055	−0.557	−10.04	0.309	−19.9
4	C=O	1.505	−1.608	1.168	0.439	10.01	−0.454	94.2
	C−O	1.217	1.591	−0.976	−0.615	−9.91	0.227	−17.9
5	C=O	1.452	−1.519	1.195	0.323	9.46	−0.574	95.8
	C−O	1.270	1.575	−0.878	−0.697	−9.81	0.115	−15.6
6	C=O	1.399	−1.427	1.230	0.197	8.89	−0.724	97.8
	C−O	1.323	1.567	−0.763[d]	−0.804[d]	−9.76	−0.027	−13.1

[a] O···O distance constant at 2.722 Å and <OHO = 180°. [b] As plotted in Figure 5. [c] See definition Table I, footnote *c*; all assignments as for VI. [d] Note $q_{YY} \leftrightarrow q_{XX}$ interchange compared with 1.

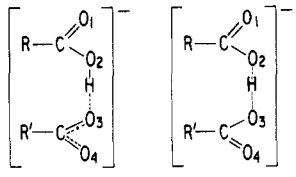

XV XVI

Figure 9. Anions in asymmetrically (XV) and symmetrically (XVI) H-bonded acid salts.

and III), and this assessment is confirmed by the experimental results (Figure 6).

When asymmetric and symmetric H bonding in acid salts (Figure 9) are compared now, some insight into the shifts in the oxygen EFG's which accompany the gradual change in H-bonding type can be gained from inspection of some theoretical results[42] for the model H-bonded formic acid dimer. In this series of calculations all structural parameters other than the coordinates for the H-bonded protons were frozen: the protons were moved in concerted fashion by increments of 0.1 μ_B (~0.053 Å) along the linear H bonds.

Reference to Table IV and Figure 5 shows that a progressive shift in H-bond character from asymmetric to symmetric is accompanied by regular changes in the ^{17}O e^2qQ/h and η values for both the C=O··· and O—H··· groups: for the C=O··· group the shift is to lower e^2qQ/h and higher $|\eta|$ values, while for the O—H··· group the shift is to lower $|e^2qQ/h|$ and lower η values. Also the orientations of the PA's of the two oxygens are becoming more similar. Thus it can be noted that the orientation of the Y axis for the C=O··· oxygen at point 6 is ~+8° while that of the Z axis for the O=H··· oxygen is ~−13°: that these orientations have the same sense with respect to the molecular framework can be seen by inspection of Figure 4 (VI). The studies for the fully symmetric ($HCOOD_2$) dimer with relaxed geometry,[40] together with arguments advanced below, suggest a $Z \leftrightarrow Y$ interchange for the symmetrically H-bonded C=O··· oxygen compared with that for the asymmetric case.

Collation of the preceding experimental and theoretical information allows a correspondence scheme to be deduced which describes the gradual shifts in the oxygen coupling constant values, assignments and orientations accompanying a continuous change from asymmetric to symmetric H bonding. The scheme is represented diagrammatically in Figure 10 where, for convenience, the example is that of a doubly H-bonded carboxylic acid dimer. A similar scheme would obtain for the acid salts: here the C=O group would be replaced by the carboxylate C—O group while the scheme would describe changes only for the two oxygens participating in the H bond (O_2 and O_3 in Figure 9).

In Figure 10 the orientation of the oxygen q_{ZZ} axis in the symmetric H bond is predicted to be approximately coincident with the C—O bond; i.e., $\theta \simeq 0°$. More specifically, the experimental evidence discussed below and also the results of the formic acid calculations suggest a θ value closer to −10° (sign convention as for the OH group). The θ value might be expected to depend on the local symmetry of the oxygen nucleus, particularly on the O···H···O and C−O···H angles and the degree of planarity of the H bond. The results for the formic acid dimer in Table IV refer to a fully planar molecule with O···H···O angles of 180°: however, the previous study[4] established that the orientations of both the H-bonded carboxyl and hydroxyl oxygen PA's were very similar for the fully planar gaseous dimer and for the crystal system consisting of essentially planar monomers H bonded at ~80° to form an infinite chain.[39] Where experimental data are available, the O···H···O angle appears close to 180°,[25] e.g., 175.4 (4)° for potassium hydrogen chloromaleate[28] and 176 (2)° for sodium hydrogen diacetate.[36] The available experimental data relevant to the present discussion are limited to the preliminary observations on potassium hydrogen maleate by Poplett et al.[43] Their results suggested a negative sign for the coupling constant of the symmetrically H-bonded oxygen and an angle of q_{ZZ} with the O···H bond of ~±60°: with use of the experimental C−O···H angle of 109.3 (2)° of the X-ray structure,[27b] a θ angle (consistent with the definitions in Figure 10 and Table III) of either −10° or −130° can be calculated.

Grouping of ^{17}O Values for Symmetric H Bonds. This question is approached from two directions. First, it is approached by exploring the ^{17}O behavior for pairs of compounds having very similar intramolecular structure but exhibiting both symmetric and asymmetric H bonding: for this purpose data for the pairs maleic acid/potassium hydrogen maleate (**15** and **27**), benzoic acid/potassium hydrogen dibenzoate (**1** and **30**), *p*-chlorobenzoic acid/potassium hydrogen bis(*p*-chlorobenzoate) (**2** and **31**), *m*-chlorobenzoic acid/potassium hydrogen bis(*m*-chlorobenzoate) (**3** and **32**), and aspirin/potassium hydrogen diaspirinate (**7** and **33**) are available. Experimental difficulties have hampered the collection of ^{17}O data for chloromaleic acid.[52] And second it is approached by examination of data for symmetrically and asymmetrically H-bonded acid salts. For the discussion to be facilitated, some structural parameters from diffraction experiments are collected in Table V.

(26) Almenningen, A.; Bastiansen, O.; Motzfeldt, T. *Acta Chem. Scand.* **1970**, *24*, 747–748.
(27) (a) Darlow, S. F.; Cochran, W. *Acta Crystallogr.* **1961**, *14*, 1250–1251. (b) Darlow, S. F. *Ibid.* **1961**, *145*, 1257–1259.
(28) Ellison, R. D.; Levy, H. A. *Acta Crystallogr.* **1965**, *19*, 260–268.
(29) Skinner, J. M.; Stewart, G. M. D.; Speakman, J. C. *J. Chem. Soc.* **1954**, 180–184.
(30) Mills, H. H.; Speakman, J. C. *J. Chem. Soc.* **1963**, 4355–4363.
(31) Macdonald, A. L.; Speakman, J. C. *J. Chem. Soc., Perkin Trans. 2* **1972**, 1564–1566.
(32) Sequeira, A.; Berkebile, A.; Hamilton, W. C. *J. Mol. Struct.* **1967**, *1*, 283–294.
(33) Okaya, Y. *Acta Crystallogr.* **1965**, *19*, 879–882.
(34) Einspahr, H.; Marsh, R. E.; Donohue, J. *Acta Crystallogr., Sect. B* **1972**, *B28*, 2194–2198.
(35) Thomas, J. O. *Acta Crystallogr., Sect. B* **1973**, *B29*, 1767–1776.
(36) Barrow, M. J.; Currie, M.; Muir, K. W.; Speakman, J. C.; White, D. N. J. *J. Chem. Soc., Perkins Trans. 2* **1975**, 15–18.
(37) Larsson, G.; Nahringbauer, I. *Acta Crystallogr., Sect. B* **1968**, *B24*, 666–672.

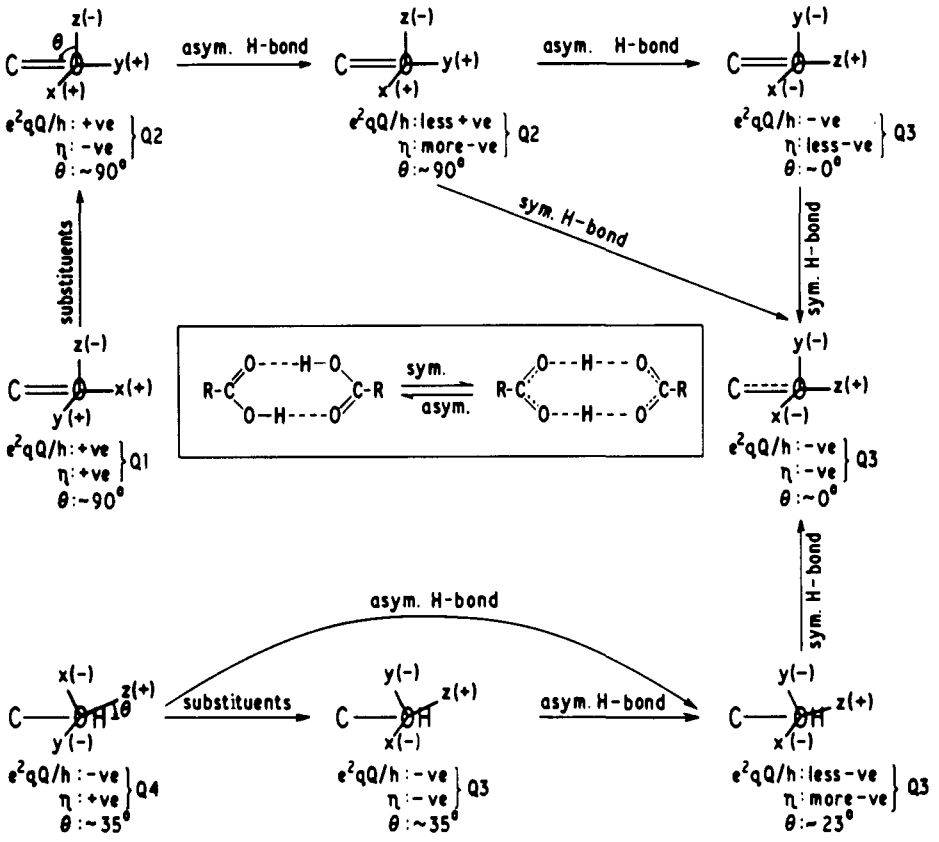

Figure 10. Schematic representation of the relationships between the EFG's of oxygens involved in H-bonding in a doubly H-bonded carboxylic acid dimer. *Q*1, *Q*2, etc. refer to quadrants in Figure 6. The signs of the EFG components are shown in brackets.

Table V. Comparison of Bond Lengths for Symmetric and Asymmetric H Bonds

compd	O···O, Å	symm?	C–O (1,4),[a] Å	C–O (2,3),[a] Å	O-H···[Å]	ref[b]
potassium hydrogen maleate (**27**)	2.437 (4)	√	1.235 (2)	1.284 (3)	(1.219)	27 (X)
maleic acid (**15**)	2.502 (2)	X	1.218 (2)	1.304 (2)	0.91 (2)	45 (X)
			1.300 (2)[c]	1.222 (2)		
potassium hydrogen chloromaleate (**29**)	2.403 (3)	√	1.226 (2)	1.277 (3)	1.206 (5)	28 (N)
			1.240 (2)	1.280 (3)	1.199 (5)	
potassium hydrogen dibenzoate (**30**)	2.51 (4)	√	1.22 (4)	1.24 (4)	(1.26)	29 (X)
benzoic acid (**1**)	2.64	X	1.24 (1)[e]	1.29 (1)[e]	*d*	50 (X)
potassium hydrogen bis(*p*-chlorobenzoate) (**31**)	2.457 (13)	√	1.225 (13)	1.321 (13)	(1.229)	30 (X)
p-chlorobenzoic acid (**2**)	2.615 (5)	X	1.253 (6)[e,f]	1.273 (6)[e,f]	1.11 (12)	48 (X)
potassium hydrogen bis(*m*-chlorobenzoate) (**32**)	2.437 (6)	√	1.223 (6)	1.290 (6)	(1.219)	31 (X)
m-chlorobenzoic acid (**3**)	2.662	X	1.222 (6)[e]	1.304 (6)[e]	0.92 (4)	49 (X)
potassium hydrogen diaspirinate (**33**)	2.448 (4)	√	1.217 (4)	1.284 (2)	1.224 (2)	32 (N)
aspirin (**7**)	2.645	X	1.235 (4)[e]	1.287 (4)[e]	1.12 (7)	51 (X)
potassium hydrogen phthalate (**25**)	2.546	X	1.210 (7)	1.305 (6)	0.88	33 (X)
			1.232 (6)	1.269 (6)		
phthalic acid (**11**)	2.684	X	1.225[e]	1.303[e]	*d*	53 (X)
potassium hydrogen oxalate (**24**)	2.523 (2)	X	1.211 (2)	1.308 (2)	0.87 (2)	34 (X)
			1.234 (2)	1.256 (2)		
β-oxalic acid (**13**)	2.674 (2)	X	1.222 (1)[e]	1.290 (1)[e]	0.95 (2)	46 (X)
(hydrazinium hydrogen oxalate)	(2.457 (1))	√	(1.224 (1))	(1.279 (1))	((1.229))	(35 (X))
(sodium hydrogen diacetate)	(2.475 (14))	√	(1.239 (9))	(1.282 (9))	((1.236))	(36 (N))
potassium hydrogen diformate (**23**)	2.447 (6)	X	1.220 (6)	1.257 (8)	*d*	37 (X)
			1.240 (6)	1.251 (7)		
sodium formate (**26**)			2.246 (1)	2.246 (1)		38 (X)
formic acid (**19**)	2.625 (2)	X	1.221 (2)[e]	1.311 (2)[e]	0.88 (2)	39 (X)

[a] For oxygen numbering see Figure 9. [b] X ≡ X-ray diffraction; N ≡ neutron diffraction. [c] O_4 in an O–H···O group involved in intermolecular H bonding. [d] Not determined. [e] For C=O··· and O–H···oxygens, respectively. [f] Virtual equivalence an artifact of crystal disorder, see ref 48.

Considering first the acid/acid salt data, we note from Figure 6 that the ^{17}O values for all pairs (i.e., **15**/**27**, **1**/**30**, **2**/**31**, **3**/**32**, and **7**/**33**) conform to the general scheme of Figure 10 except for the O—H··· values for benzoic acid (**1**): that is, all the C=O··· and O—H··· values are shifted to the left of Figure 6 on going from asymmetric to symmetric H bonding. For the C=O··· values an additional contribution from ionization could be expected: by analogy with the formic acid/formate shift (**19**/**26** and VI/V) for the C=O group this contribution would also be expected to be to the left in Figure 6. If the magnitude of the "shifts" is assessed as the distance traversed along the C=O and O—H lines, then somewhat greater changes in the C=O··· values compared

(38) Markila, P. L.; Rettig, S. J.; Trotter, J. *Acta Crystallogr., Sect. B* **1975**, *B31*, 2927-2928.
(39) Nahringbauer, I. *Acta Crystallogr., Sect B* **1978**, *B34*, 315-318.

with the O—H··· values are evident for the asymmetric to symmetric H-bond transition for the above five examples. Here the total "shifts" for the C=O··· values are assumed to be a sum of right to left shifts on the C=O line (2nd quadrant) and left to right shifts on the O—H line (3rd quadrant). The relatively greater C=O··· shifts may possibly be accounted for by the ionization contribution and also by an intrinsically larger perturbation by H bonding.[4]

As it has been remarked that symmetric H bonds in these type A salts are both very short and of uniform length (average 2.447 (3) Å[25b]), a critical comparison of structural data may be enlightening. Reference to Table V shows that the H bonds are shorter for all the acid salts than for the acids except for the marginal case of maleic acid[54] and potassium hydrogen dibenzoate: the spread of O···O values for these five symmetric H bonds is about 0.1 Å while that for the asymmetric H bonds is somewhat greater at 0.16 Å. Some dependence of the ^{17}O values on the C—O and O—H bond lengths might also be expected. For the present sample, although four of the salts have C—O bond lengths between 1.28–1.29 Å, one (**31**, 1.32 Å), at least, is well outside this range. Some scatter is also evident for the C=O··· and C—O(—H···) bond lengths for the acids (**15**, **1**, **3**, and **7**) although for this sample it is perhaps unusually small. Therefore greater relative uniformity in the O···O and C—O bond lengths for symmetric as compared with asymmetric H bonds does not seem significant for this sample of acids/acid salts, at least. Disregarding the early X-ray data for potassium hydrogen dibenzoate which contain high esd's, potassium hydrogen chloromaleate (O···O distance) and potassium hydrogen bis(*p*-chlorobenzoate) (C—O distance) would appear to differ most from the structural average for these acid salts, but such differences are not reflected in the ^{17}O values (Figure 6). For the O—H··· bond lengths the data are more imprecise: however, the spread of values for the asymmetric H-bonded acids is clearly greater than for the salts.

It is appropriate at this point to mention vibrational effects. Rigorously, the EFG's are averages over the molecular vibrational modes not simply properties of the static structure; however, theoretical studies have found that such corrections are usually small.[2] It is expected that the weakly bound acid proton in the symmetric H bond would undergo unusually large amplitude vibrations, assuming that it is localized in a central potential and not in a double-well potential.[25] The effect of such vibrations on the ^{17}O values will depend on the relative contributions of proton terms to the total oxygen EFG tensor; these contributions are currently being investigated.[40] There is now evidence[40] that vibrational corrections to the ^{2}H coupling constants for the proton bound in a symmetric single-well potential will be very small for asymmetric stretches, at least.

The second part of this discussion concerns the asymmetrically H-bonded acid salts; the relevant diffraction data are also shown in Table V. For potassium hydrogen phthalate (**25**) and potassium hydrogen oxalate (**24**) the "differences" between the C=O··· and O—H··· values are less than those for the corresponding acids, but this could mostly be accounted for by the C=O··· shifts caused by ionization (Figure 6). Both H-bond lengths for these two salts are longer than those of the symmetrically H-bonded salts but shorter than for their corresponding acids (**11** and **13**). Note from Table V that the hydrogen oxalate iron *can* form a symmetrical H bond if in a favorable crystallographic form.[35] For potassium hydrogen diformate (**23**), however, an intermediate structure is observed; although the H bond is very short, crystallographic asymmetry prevents it from being symmetric.[37] The ^{17}O values for these H-bonded oxygens are very interesting: if it is assumed that the proper position for the C=O··· values is indeed in the 3rd quadrant (Figure 6), then the "difference" (i.e., along the O—H line) between the two oxygen values is very small. While the two values are in the same region of the graph as the ^{17}O values for the fully symmetric H bond, it is not certain that they are "converging" toward the symmetric values.

In summary then: the examination has provided no clear reason why elements of the molecular structure (e.g., substituents) other than the symmetric H bond do not cause a greater spread of the ^{17}O values. As a final point it should be noted that ^{17}O signals for the non-H-bonded carboxyl oxygens in the acids salts (O_1 and O_4 in Figure 9) were not detected in the studies of Poplett and Smith,[13,52] although some such signals were detected in other studies.[11,12] The availability of further data for the non-H-bonded carbonyl groups would be helpful in indicating the magnitude of substituent effects in these salts, in particular.

Some Further Examples. In addition to the example of the H-bonded and non-H-bonded carbonyl groups in phthalimide noted at the beginning of this section, there are two other experimental examples which lend support to the H-bonding-induced trends depicted in Figure 10. Oxalic acid occurs in two distinct crystalline forms, α (**16**) and β (**13**), which exhibit different H-bonding structure: consideration of the H-bond length and other factors lead to the conclusion that H bonding is stronger in the β modification (O···O = 2.674 (2) Å, ∠O–H···O = 174 (2)°) than in the α form (O···O = 2.702 (1) Å, ∠O–H···O = 146.0 (8)°).[46] This assessment is in accord with the experimental e^2qQ/h and η values for both the C=O and OH groups as shown in Figure 6; i.e., both sets of values are shifted to the left of the diagram for the β form in conformity with the general scheme in Figure 10. In crystalline maleic acid there are two types of H bond, one intramolecular (O···O = 2.502 (2) Å, ∠O–H··· = 171 (2)°) and the other intermolecular (O···O = 2.643 (2) Å, ∠O–H···O = 178 (2)°).[45] The NQDR data[21] indicate four distinct oxygen nuclei (**14** and **15**), two each from C=O··· and O—H··· groups. While these resonances have not been assigned to particular H-bond types, the present arrguments would predict that the values represented by points **14** refer to the oxygens involved in the intermolecular H bond, while points **15** arise from the intramolecularly H-bonded oxygens. Note that different assignments involving an $X \leftrightarrow Y$ interchange are predicted for the two C=O··· values as plotted in Figure 6. For isophthalic acid (**12**) the crystal structure[55] again shows two different intermolecular H bonds with unexpectedly large differences in the O···O distances (2.682 and 2.581 Å), yet signals from only two oxygen nuclei, not four, were detected.[16]

Other Oxygen Groups

Although the bulk of the experimental and theoretical ^{17}O data is for carbonyl and hydroxyl groups, a few results for oxygen in other bonding arrangements are available. Cheng and Brown[12] have assigned ^{17}O values to noncarbonyl oxygens in benzoyl peroxide (**44**), benzyl chloroformate (**45**), phenyl benzoate (**47**), benzoic anhydride (**48**), phthalic anhydride (**49**), maleic anhydride (**50**), chloroacetic anhydride (**51**), and phthalide (**53**), while an ether oxygen (xanthene (**65**)) has also been detected.[9] Experimental data[11] for oxygen bonded to nitrogen, phosphorus, or sulfur are not considered here. Useful theoretical results are limited to

(40) Gready, J. E.; Bacskay, G. B.; Hush, N. S., to be submitted for publication.
(41) Smith, R. A. *Acta Crystallogr., Sect. B* **1975**, *B31*, 2347–2348.
(42) Full computational details and results for relaxed geometries are reported in ref 40.
(43) Poplett, I. J. F.; Sabir, M.; Smith, J. A. S., unpublished results.
(44) Harvey, J. S. M. *Proc. R. Soc. London, Ser. A* **1965**, 285, 581–596.
(45) James, M. N. G.; Williams, G. J. B. *Acta Crystallogr., Sect. B* **1974**, *B30*, 1249–1257.
(46) Derissen, J. L.; Smit, P. H. *Acta Crystallogr., Sect. B* **1974**, *B30*, 2240–2242.
(47) Sax, M.; McMullan, R. K. *Acta Crystallogr.* **1967**, *22*, 281–288.
(48) Miller, R. S.; Paul, I. C.; Curtin, D. Y. *J. Am. Chem. Soc.* **1974**, *96*, 6334–6339.
(49) Gougoutas, J. Z.; Lessinger, L. *J. Solid-State Chem.* **1975**, *12*, 51–62.
(50) Sim, G. A.; Robertson, J. M.; Goodwin, T. H. *Acta Crystallogr.* **1955**, *8*, 157–164.
(51) Wheatley, P. J. *J. Chem. Soc.* **1964**, 6036–6048.
(52) Poplett, I. J. F., private communication, 1980.
(53) Nowacki, W.; Jaggi, H. *Z. Kristallogr.* **1957**, *109*, 272–283.
(54) **15** is taken to represent the *intramolecular* H bond: see later discussion.
(55) Derissen, J. L. *Acta Crystallogr., Sect. B* **1974**, *B30*, 2764–2765.

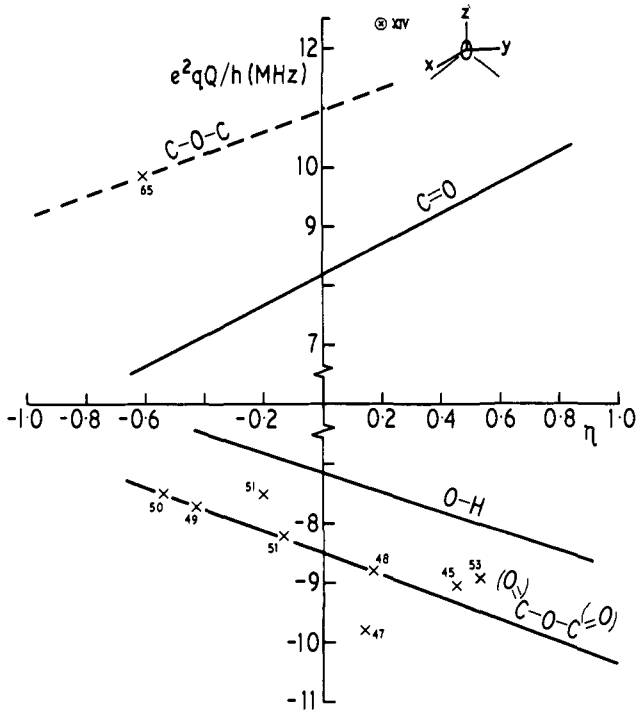

Figure 11. e^2qQ/h vs. η graph for single-bonded oxygen. × represents experimental points and circled × a theoretical value.

those for ethylene oxide (XIV) and hydrogen peroxide (XVIII).[1]

Except for the peroxides which are discussed separately, the data are plotted in Figure 11. Despite the scarcity of data this plot bears some similarities to that for the carbonyl group. It is apparent from Figure 11 that the oxygen values for the non-H-bonded C–O–C group in the anhydrides and esters cover a considerable range. They were assigned negative e^2qQ/h values arbitrarily, and no attempt at assignments or orientations has been made.

The theoretical assignment and orientation for ethylene oxide (XIV) are given in Figure 4; the orientation is determined purely by high molecular symmetry. Calculated values[1] for XIV are q_{zz} = −2.614 au and η = 0.119; a scaled value for e^2qQ/h of ~+12.4 MHz is calculated. A tentative correlation of these theoretical results with the xanthene (XVII) experimental values[9] is given

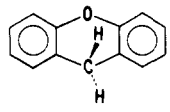

XVII

in Figure 11. It may be significant that the absolute values of the slopes of the OH and (O)=C—O—O=(O) lines are both ~1.8 MHz/unit of η while the corresponding value for the C=O line is ~2.4 MHz.

Peroxides. Although a very close analogy in electronic and geometric structure between hydrogen and benzoyl peroxides would not be expected, the experimental and theoretical e^2qQ/h and η values show suprising similarities. The EFG assignment and orientation for H_2O_2 have been calculated from data given in ref 1 and are shown in XVIII. In the original $\{x, y, z\}$ molecular axis system, O_1 and O_2 are on the z axis while H_2 is on the yz

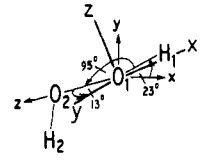

XVIII

plane. The dihedral angle is ~115°.[56] As shown in the sketch the Y axis of the PA system is rotated ~13° from the z axis while the projection of the X axis onto the xy plane places it almost coincident with the O–H bond direction. The computed q_{ZZ} and η values are −3.027 au and 0.981, respectively. A scaled theoretical value of +14.3 MHz is calculated. The crystal structure of benzoyl peroxide[47] shows a number of structural differences about the peroxide bond compared with H_2O_2, the chief being a dihedral angle of only ~91°; the O–O distances are, however, very similar −1.460 (15) and 1.475 Å, respectively. The experimental e^2qQ/h and η values for the peroxide oxygen of benzoyl peroxide are ±11.916 (2) MHz and 0.987 (1).[12] Thus when a solid-state effect of similar magnitude to those previously discussed is allowed, it can be prediced that the assignments of the PA system for the peroxide oxygen in benzoyl peroxide are either as given in XVIII or with a $Z \leftrightarrow Y$ interchange (i.e., e^2qQ/h = −11.916 MHz), although some difference in the orientation can be expected.

Conclusions and Future Directions. A general scheme for correlating assignments and orientations of the electric field gradient principal axis systems of given nuclei in molecules has been illustrated for oxygen in organic compounds. While the available experimental and theoretical data are in good accord with the scheme, the discussion has identified several areas where lack of data precludes a definite assessment of its generality. As the bulk of the available ^{17}O NQR results are for H-bonded carbonyl and hydroxyl groups in carboxylic acids, a need exists for further data on these groups in non-H-bonded compounds and for oxygen in other functional groups such as ethers. Further ab initio calculations on O-containing organic molecules are required to establish the range of possible assignments, orientations, and magnitudes of the oxygen EFG components and to differentiate the effects of changes in bonding structure caused by altering substituents or by forming H bonds under conditions where variable solid-state perturbations are absent. Experimental ^{17}O results for a wider range of symmetrically H-bonded acid salts would help to resolve the problems raised in Effects of H Bonding.

Acknowledgment. The author thanks Dr. I. Poplett and D. Edmonds, Mr. S. Brosnan, and Professor J. A. S. Smith for helpful discussions on experimental matters and permission to use their unpublished results. Calculations on the formic acid dimer were performed by using the Cyber-73 computer from the University of Sydney.

Note Added in Proof: The NQDR results for **1–13** have now been published;[20] note that the results for β-oxalic acid are T dependent. Also, the NQDR results for the acid salts **23–25** and **30–33** together with new results for the symmetrically H-bonded compounds quinolinic acid and imidazolium hydrogen maleate are in the course of publication:[57] these new results conform well to the correlation graph Figure 6. New NQDR results for methanol[58] also conform well to Figure 6.

(56) Redington, R. L.; Olson, W. B.; Cross, P. C. *J. Chem. Phys.* **1962**, *36*, 1311–1326.
(57) Poplett, I. J. F.; Smith, J. A. S., *J. Chem. Soc., Faraday Trans. 2*, submitted.
(58) Brett, C.; Edmonds, D. T., private communication, 1981.